Chemokine receptor: directed imaging and therapy

Andreas K. Buck, Antje Stolzenburg, Heribert Hänscheid, Andreas Schirbel, Katharina Lückerath, Margret Schottelius, Hans-Jürgen Wester, Constantin Lapa

Angaben zur Veröffentlichung / Publication details:

Buck, Andreas K., Antje Stolzenburg, Heribert Hänscheid, Andreas Schirbel, Katharina Lückerath, Margret Schottelius, Hans-Jürgen Wester, and Constantin Lapa. 2017. "Chemokine receptor: directed imaging and therapy." *Methods* 130: 63–71. https://doi.org/10.1016/j.ymeth.2017.09.002.

Chemokine receptor – Directed imaging and therapy

Andreas K. Buck [a,*], Antje Stolzenburg [a], Heribert Hänscheid [a], Andreas Schirbel [a], Katharina Lückerath [a], Margret Schottelius [b], Hans-Jürgen Wester [b], Constantin Lapa [a]

[a] *Department of Nuclear Medicine, University Hospital Würzburg, Germany*
[b] *Technische Universität München, Walther-Meißner-Str. 3, 85748 Garching, Germany*

Contents

* Corresponding author at: Dept. of Nuclear Medicine, University Hospital Würzburg, Oberdürrbacherstr. 6, D-97080 Würzburg, Germany.
E-mail address: buck_a@ukw.de (A.K. Buck).

1. Introduction

Chemokine receptors play an essential role during migration of immune cells towards an increasing gradient of chemokines. Binding of its natural ligand CXCL12 (SDF-1α) to the receptor results in the activation of several downstream signaling pathways, including PI3K/AKT, ultimately resulting in gene expression and protein translation [1]. CXCR4 plays a pivotal role in embryonic development, enabling the migration of progenitor cells before differentiating into organs and tissues at their final destination [2]. The CXCR4/CXCL12 axis also has numerous physiological roles in infection control and immunity.

In pathological conditions, the receptor plays a relevant role in tumorigenesis, enhancing cellular proliferation and invasion as well as migration of metastatic tumor cells [3]. In addition to tumor cells, CXCR4 positive bone marrow derived progenitor cells can be recruited to the tumor site, further contributing to the formation of the neovasculature in the tumor stroma. A variety of compounds has been developed to interfere with the CXCR4/CXCL12 axis. The first drug designed for human use is the bicyclam-based antagonist AMD 3100 which blocks the binding pocket of CXCR4 [4]. It has been shown that AMD 3100 induces the mobilization of $CD34^+$ hematopoietic stem cells from their niche in the bone marrow [5]. In 2008, this pharmaceutical has been approved in the U.S. and in 2009 in the European Union for mobilizing and harvesting hematopoietic stem cells prior to autologous stem cell transplantation.

More recently, peptidic antagonists and monoclonal antibodies designed to specifically inhibit CXCR4 have been developed. As an example, the human antiCXCR4 antibody BMS-936564/MDX-1338 is currently under evaluation in a clinical phase I-trial. In preclinical experiments, targeting of CXCR4 resulted in blocking of metastases [6]. The ligand to CXCR4 is expressed also in the microenvironment of tumors including stromal cells, further promoting tumor growth in an autocrine/paracrine fashion [7]. Furthermore, CXCR4 mediates proliferation and invasiveness, as

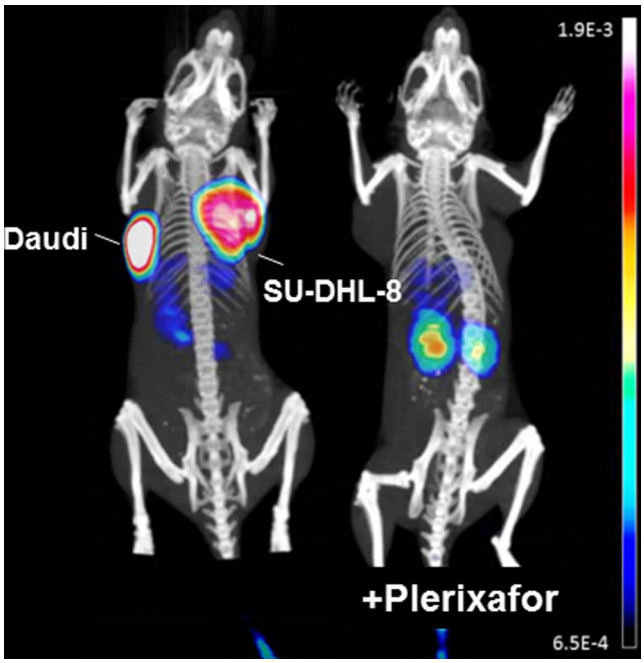

Fig. 2. Coronal μPET/CT maximum intensity projections depict CXCR4-expressing Daudi and SU-DHL-8 lymphoma xenotransplants after injection of [^{68}Ga]Pentixafor (left). For competition (right), [^{68}Ga]Pentixafor was coinjected with the CXCR4 specific ligand AMD3100 (non-specific bladder activity blanked out) This research was originally published in J Nucl Med 2011;52:1803–10 [13].

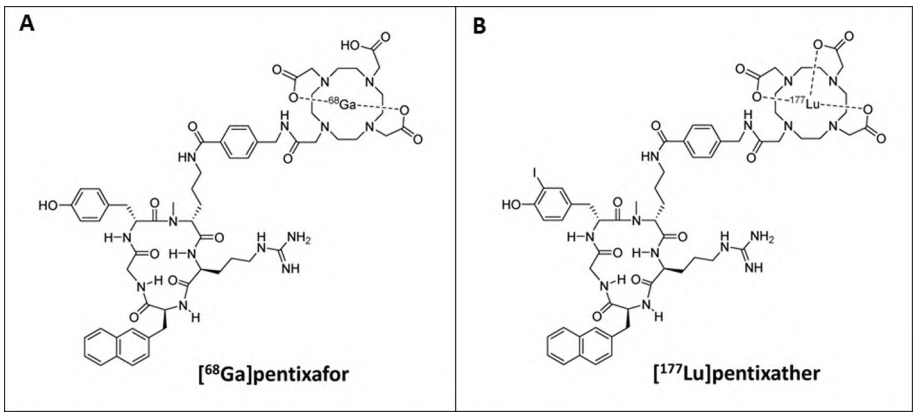

Fig. 1. A) Structure of Pentixafor (CPCR4-2). The molecule consists of the binding moiety, the linker and the chelator for trapping of the radioisotope (^{68}Ga). B) Structure of the therapeutic analog Pentixather which is suitable for labeling with the ß-emitting radioisotopes ^{90}Y and ^{177}Lu.

shown in breast cancer cells [8]. CXCL12 may also attract CXCR4$^+$ inflammatory, vascular and stromal cells to the tumor, supporting tumor growth by secreting growth factors, cytokines and proangiogenic factors.

Under physiological conditions, CXCR4 sustains the binding of CXCL12 expressing stem cells. In the pathological condition, leukemic blasts and other tumor cells which localize in the CXCL12 positive bone marrow niche can be mobilized by disrupting the CXCR4/CXCL12 axis, inducing sensitivity to anticancer drugs and radiation [9,10]. Currently, clinical trials are underway, combining the targeted approach of CXCR4 to the established concept of inhibiting angiogenesis (antiVEGF, e.g. bevacizumab) and immune checkpoints such as the programmed death receptor PD1 (nivolumab) or PD-L1 (durvalumab).

Given the relevance of the CXCR4/CXCL12 axis particularly for clinical applications in oncology, a variety of strategies have been developed, enabling the non-invasive imaging of CXCR4 using receptor directed probes. Consequently, CXCL12 conjugates have been fluorescence labeled and radiolabeled with radioisotopes including ^{99m}Tc, ^{11}C, ^{64}Cu and ^{18}F [11]. At TUM, the cyclic pentapeptide [^{68}Ga]Pentixafor which is based on the scaffold cyclo (D-Tyr^1-[NMe]-D-Orn^2-Arg^3-2-Nal^4-Gly^5 has been developed for use with positron emission tomography (Figs. 1 and 2) [12,13]. In addition, a therapeutic analog facilitating radionuclide based treatment of CXCR4$^+$ tumors has been made available (Pentixather) [14]. Here, we report on established clinical and preclinical imaging protocols and corresponding results based on a Pentixafor/Pentixather theranostic approach (Fig. 1).

2. Methods

2.1. In-vitro assays

2.1.1. CXCR4 expression analysis in cell culture experiments via flow cytometry

In the past, we have focused on CXCR4 expression in hematological neoplasms and utilized FACS analyses for quantification of protein expression in vitro. For this purpose, the human multiple myeloma cell lines OPM-2 (DSMZ No. ACC50) and MM.1S (ATCC CRL-2974) are cultured in RPMI 1640 supplemented with 10% FCS, 2 mM L-glutamine, 1 mM sodium pyruvate, 100 U/ml penicillin, and 100 lg/ml streptomycin [15]. Cells are maintained at 37 °C in a 5% CO_2 humidified atmosphere. All media and supplements are obtained from Invitrogen (Darmstadt, Germany). Single myeloma cell suspensions are stained with fluorochrome conjugated antibodies against hCXCR4-PE (hCD184; clone 12G5; Miltenyi, Bergisch-Gladbach, Germany) or other antibodies and analyzed with a BD FACSCalibur flow cytometer [16]. All samples are then analyzed in at least triplicates and are corrected concerning background with an isotype antibody. For treatment experiments myeloma cell suspensions are exposed to different substances over a period of 48 h followed by a flow cytometric analysis. Afterwards geometric mean fluorescent intensity (GeoMean) is quantified by using BD CellQuest software (Beckton Dickinson, Heidelberg, Germany).

2.1.2. Radiosynthesis of [^{68}Ga]Pentixafor for in-vitro assays and imaging

Synthesis of [^{68}Ga]Pentixafor can be performed by a fully automated, GMP-compliant procedure using a GRP synthesis module (Scintomics, Fürstenfeldbruck, Germany) connected to a ^{68}Ge/^{68}Ga generator (Eckert and Ziegler, Berlin, Germany) and equipped with a disposable single-use cassette kit (ABX, Radeberg, Germany) [17]. The eluate ([^{68}Ga]$GaCl_3$ in 0.1 M HCl) of the generator is transferred to a cation exchange cartridge, eluted with 5 N NaCl, added to a solution of 20 µg Pentixafor (Scintomics, Fürstenfeldbruck, Germany) in HEPES-buffer and heated for 6 min at 125 °C. Subsequently, the product is immobilized on a SepPak C18 cartridge, and washed with water und eluted with ethanol/water 50/50. The eluate is then passed through a sterile filter (0.22 µm) into a sterile vial und diluted with phosphate buffer solution to a total volume of 15 mL. Radiochemical purity is determined by gradient high performance liquid chromatography and thin-layer chromatography. Additionally, the product is also tested for ethanol content, pH, radionuclide purity, sterility, and endotoxins.

In the future, it can be expected that labeling of pentixafor with ^{99m}Tc will become available, because single photon emission computed tomography (SPECT) and planar scintigraphy provides a valuable alternative to PET imaging. In contrast, labeling of Pentixafor with F-18 makes only sense if used in a large number of patients.

2.1.3. In-vitro binding assay for [^{68}Ga]Pentixafor

Sub-confluent OPM-2 and MM.1 S myeloma cells are harvested and adjusted to ~4×10^5 cells/500 µl PBS per sample. Subsequently, all samples are incubated with 1×10^6 counts (28,7 kBq) per minute (cpm) [^{68}Ga]Pentixafor/50 µl PBS (~1 nM peptide/sample) for different time points. Binding or uptake is stopped by putting samples on ice for at least 2 min. After two washing steps with PBS to remove the unbound radiotracer (centrifugation, 3500 U/min, 4 °C, 2 min), binding of [^{68}Ga]Pentixafor to myeloma cells is quantified using a gamma counter (Wallac 1480-Wizard, Perkin-

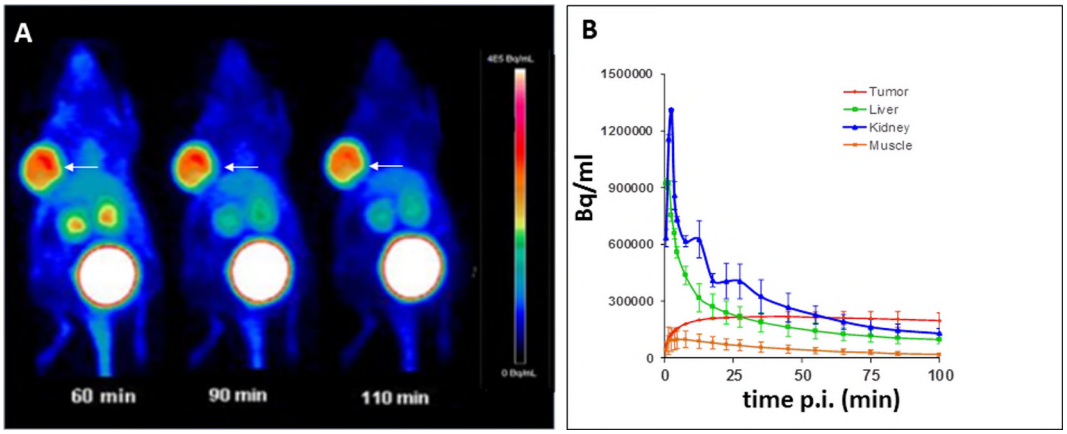

Fig. 3. A) Dynamic [^{68}Ga]Pentixafor PET imaging in an OH-1 SCLC tumor xenotransplant model. Rapid accumulation in the tumor xenotransplant (arrows) can be seen, reaching a plateau after 25 min; on the contrary, an efflux kinetic is obvious in the excreting organs liver and kidney (B) [12].

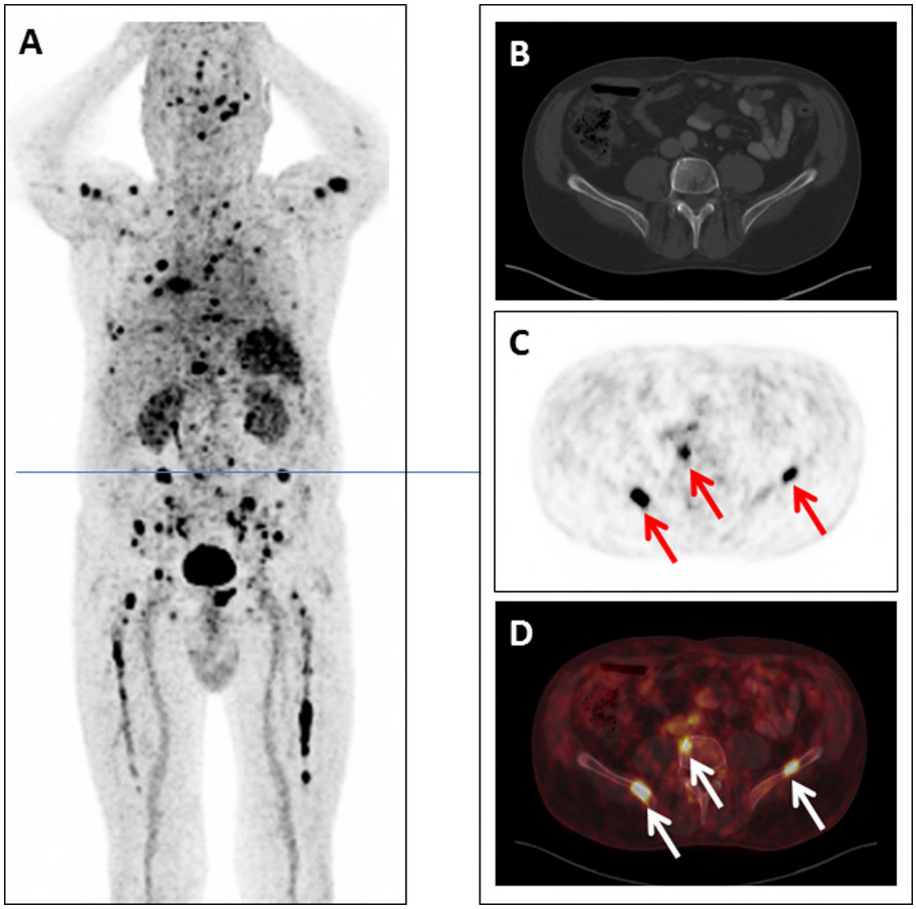

Fig. 4. A) Whole-body view of [^{68}Ga]Pentixafor PET/CT (60 min p.i.) in a patient with multiple myeloma. Multiple hot spots can be detected in the skeleton (in the ribs, long bones and the pelvis), implicating high focal CXCR4 expression in myeloma lesions. Tomographic sections of the pelvis are shown on the right with only minimal bone destruction visible at spiral CT (B). Intense focal CXCR4-expression in skeletal structures can be seen at tomographic PET section (C, arrows) and the corresponding PET/CT image (D, arrows).

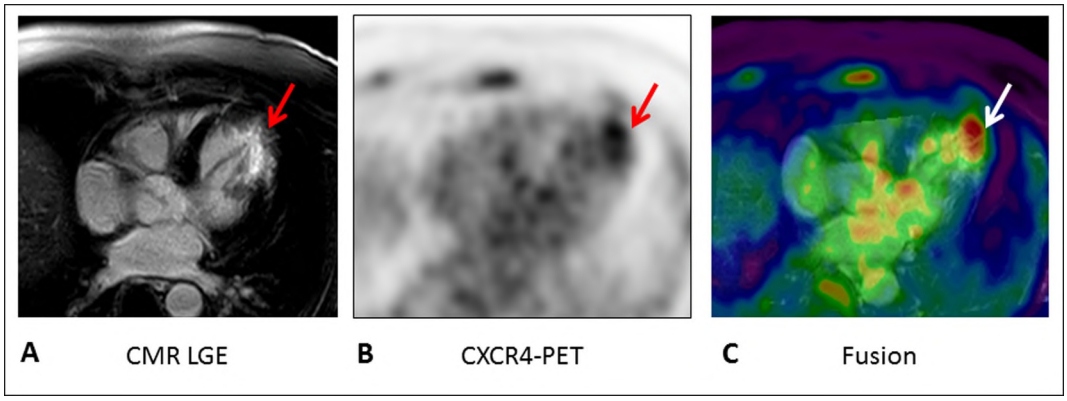

Fig. 5. A) [^{68}Ga]Pentixafor PET/CT (60 min p.i.) in a patient with ischemic heart disease. With cardiac magnetic resonance, the infarcted myocardial area in the lateral wall and the apex can be visualized by late gadolinium enhancement (arrow). The corresponding sections of [^{68}Ga]Pentixafor PET (B) and [^{68}Ga]Pentixafor PET/CT (C) show intense CXCR4-expression, indicating the presence of inflammatory, CXCR4^{+} leukocytes in the infarct area.

Elmer, Rodgau, Germany). All samples are measured in triplicates and corrected for background activity and radioactive decay. If competitive experiments are planned [15], myeloma cell lines are pretreated for 30 min with AMD3100 (100 μM; Selleck Chemicals, Houston, TX, USA) before [^{68}Ga]Pentixafor uptake analysis is performed. A similar procedure has been used for other cell types including transfected and non-transfected glioblastoma cells [18].

2.2. Preclinical imaging of CXCR4 expression with [^{68}Ga]Pentixafor and μPET

Imaging of CXCR4 expression has been performed in various animal models. A common approach to study the biodistribution of CXCR4-directed imaging biomarkers such as [^{68}Ga]Pentixafor is the use of tumor xenotransplant models (Figs. 2 and 3). For

implantation of myeloma xenotransplants, a total amount of $\sim 5 \times 10^6$ MM.1S or OPM-2 cells/100 μl PBS is injected subcutaneously in the shoulder region or the flank of immunodeficient NOD/SCID mice (NOD.CB17-*Prkdc*^{scid}/NCrHsd; Envigo, Germany). It is advisable to use younger animals (6–10 weeks) due to higher amounts of growth hormones, further promoting tumor engraftment. Mice of the same size and age are randomly distributed to experimental groups. Tumor growth should be checked and recorded daily by using a caliper. PET scans of xenotransplant bearing NOD/SCID mice are performed when the tumor reaches a size of ~200–300 mm^3 [15]. [^{68}Ga]Pentixafor is applied via tail vein injection at an activity dose of ~2.5 MBq in 100 μl PBS without using anaesthesia. After an accumulation of the tracer for 60 min, mice are put on a heating bed and a 15 min static PET scan (Inveon, Siemens Medical Solutions, Erlangen, Germany) is performed. Prior to the start of emission scanning, mice are anesthetized with 2% isoflurane using a veterinary anesthesia system (Vetland Medical, Louisville, KY, USA). After decay and washout of [^{68}Ga]Pentixafor, a PET scan with a second radiotracer can be carried out. As described for [^{68}Ga]Pentixafor, e.g. [^{18}F]FDG (~9 MBq/100 μl) is administered via tail vein injection. PET scanning is also performed 1 h post-injection for 15 min. For competitive experiments, AMD3100 (mice 2 mg/kg body weight, rats 30 mg/kg body weight [19]) is administered intravenously immediately before [^{68}Ga]Pentixafor [15] or ~30 min subcutaneously before [^{68}Ga]Pentixafor injection (Fig. 2) [19]. A similar procedure for [^{68}Ga]Pentixafor PET scanning is also possible in various xenograft animal models including glioma, and osterosarcoma [19,20].

All tumor lesions are imaged using a small-animal PET scanner (Inveon, Siemens Medical Solutions, Erlangen, Germany) and images are reconstructed using an ordered subset expectation maximization 2D (OSEM 2D) algorithm. Mean tumor-to-background ratios (TBR) are determined by drawing a volume of interest (VOI; $3 \times 3 \times 3$ pixels) around individual tumor lesions and healthy soft tissue in the contralateral flank (background) using 'A Medical Image Data Analysis Tool' (AMIDE) software (http://amide.sourceforge.net/) [16].

2.3. CXCR4-directed PET imaging of CXCR4 expression in humans

To fully exploit the advantages of integrated molecular and anatomical imaging, use of an integrated PET/CT scanner is recommended. (Figs. 4 and 5). The optimal time point for static [^{68}Ga]Pentixafor PET/CT imaging has been shown to be between 30 min and 60 min after i.v. injection of 100–150 MBq [^{68}Ga]Pentixafor [21–23]. Prior to CXCR4-directed PET/CT, no particular patient preparation (e.g., fasting or premedication) is needed. Corresponding CT scans for attenuation correction can be acquired using a low-dose CT protocol (20 mAs, 120 keV, 512×512 matrix, 5 mm slice thickness, increment of 30 mm/s, rotation time of 0.5 s, and pitch index of 0.8) including the base of the skull to the proximal thighs. Alternatively, contrast-enhanced spiral CT (dose modulation with a quality reference of 210 mAs) can be acquired in selected patients. Consecutively, PET emission data are acquired in three-dimensional mode with a 200×200 matrix with 2–3 min emission time per bed position. After decay and scatter correction, PET data are reconstructed iteratively with attenuation correction.

2.3.1. Visual interpretation of [^{68}Ga]Pentixafor-PET

Physiological uptake of [^{68}Ga]Pentixafor can be observed in the kidneys, in the bladder, the adrenals, and, to varying degrees, in the bone marrow and the spleen (Fig. 4) [21]. It is recommended that all CT scans are scored by a board-certified radiologist, and all PET scans are scored by a board-certified nuclear medicine physician. All PET scans are analyzed, i.e. in case of multiple myeloma, for the presence of areas with focally increased tracer uptake within the skeleton (i.e., more intense compared to surrounding normal bone marrow (BM) uptake excluding articular processes, with or without any underlying lesion identified by CT) or in tissues with usually mild or homogenous radionuclide accumulation are rated positive [15,22,24].

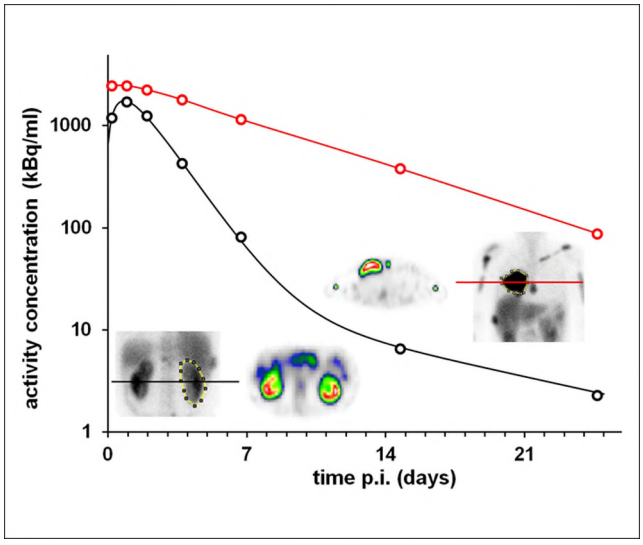

Fig. 6. Dosimetry in a patient with multiple myeloma prior to endoradiotherapy using [^{177}Lu]Pentixather. The red curve shows intense retention of the radiotracer in the right ventral chest wall (see tomographic section and planar view on the right with only moderate efflux over time). On the contrary, there is rapid metabolization of the radiotracer by the kidneys (black curve, see also tomographic sections and planar view on the left).

2.3.2. Quantification of [^{68}Ga]Pentixafor

Semi-quantitative analysis generally comprises calculation of maximum standardized uptake values (SUV_{max}) as well as SUV_{mean} by 2D ROIs with a diameter of 1.5 cm around the hottest pixel. Diffuse BM involvement is considered if the tracer uptake is diffusely increased with an SUV_{max} equal to, or greater than the uptake in the spleen.

2.4. Radiosynthesis of [^{177}Lu]Pentixather and [^{90}Y]Pentixather for dosimetry and treatment

Synthesis of [^{177}Lu]Pentixather for dosimetry is performed using a solution of 75 μg Pentixather (Scintomics, Fürstenfeldbruck, Germany) and 7 mg gentisic acid in 525 μl of a 0.4 M sodium acetate buffer solution (pH 5.2) is added to a solution of 300 MBq [^{177}Lu]$LuCl_3$ (ITG, Garching, Germany) in 200 μl 0.04 M HCl and stored in a heating block for 35 min at 100 °C. After cooling, the solution is transferred into a sterile bench, diluted with 8 ml saline and passed through a sterile filter (0.22 μm) into a sterile vial. Every single batch of [^{177}Lu]Pentixather, before release, has to be tested for radiochemical purity by gradient high-performance liquid chromatography and thin layer chromatography. Additionally, the product has to be tested for pH and a bubble point test should be performed.

Up to 8 GBq [^{90}Y]Pentixather for endoradiotherapy are prepared for therapeutic purposes in a single patient analogously to the radiosynthesis of [^{177}Lu]Pentixather. The only differences are the amount of peptide (250 μg) and the volume of the final injection solution (~15 mL saline). In the future, evaluation of Pentixather labelled with α-emitting particles such as ^{213}Bi or ^{225}Ac could be a promising approach [14].

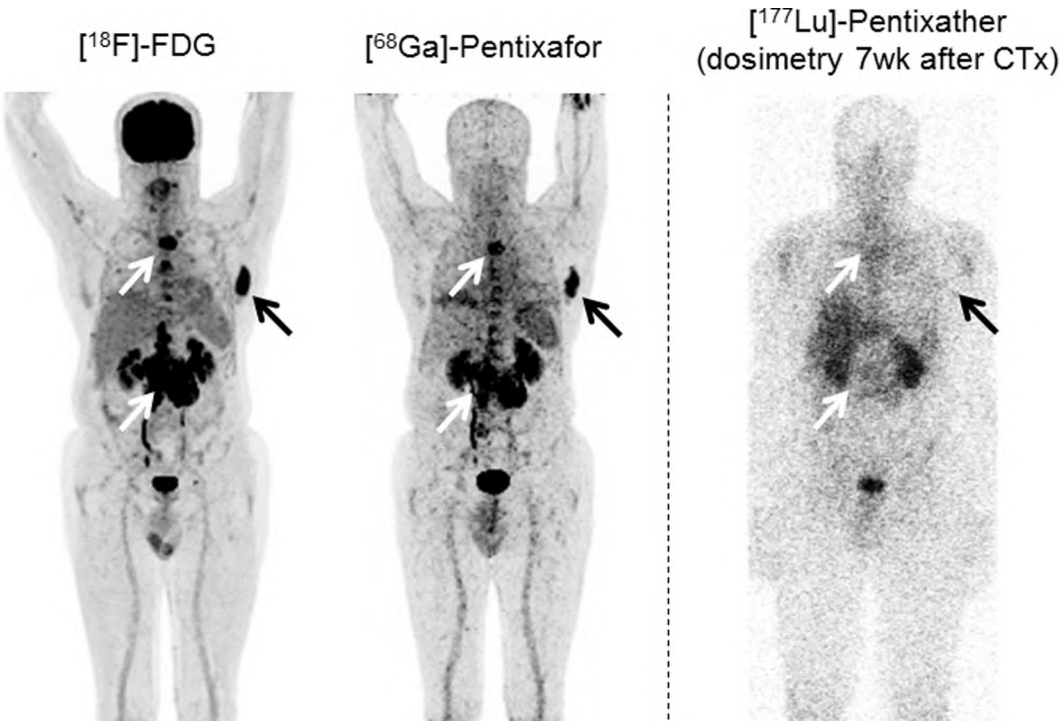

Fig. 7. Example of therapy-induced CXCR4 downregulation in a patient with advanced Multiple Myeloma with extramedullary disease. Display of maximum intensity projections (PET) and planar whole-body images derived from [^{177}Lu]Pentixather dosimetry. Initially, the patient presented with high CXCR4^{+} expression in intra- and extramedullary MM (arrows). Due to the distinct receptor expression, CXCR4-directed therapy was planned but postponed in favor of a single cycle of chemotherapy with dexa-BEAM (dexamethasone, carmustine, melphalan, cytarabine, etoposide) which resulted in no significant myeloma response. At the time point of scheduled CXCR4-directed therapy 7 weeks later, serum myeloma markers had re-gained pre-treatment values. Surprisingly, no relevant CXCR4 expression could be demonstrated during dosimetry (arrows), thus precluding CXCR4-directed endoradiotherapy.

2.5. Dosimetry prior to CXCR4-directed radionuclide therapy

When radiolabeled with α- or ß$^{-}$-emitters, the CXCR4 ligand Pentixather can be used for CXCR4-targeted radionuclide therapy. Although CXCR4 is widely overexpressed in various types of solid tumors and hematopoietic malignancies, experience with CXCR4-directed endoradiotherapy has solely been reported in the treatment of patients with multiple myeloma with ^{177}Lu- or ^{90}Y-labeled Pentixather [25,26]. As CXCR4 is normally expressed in the bone marrow, myelosuppression is the dose limiting adverse reaction in non-myeloablative treatment. When high activities of ^{177}Lu- or ^{90}Y-labeled Pentixather are used for myeloablation in combination with chemotherapy and autologous stem cell transplantation, usually the kidneys represent the dose limiting organ. Similar to other peptide receptor radionuclide therapies, activity is retained in the renal parenchyma, potentially evoking impairment of the kidney function due to local irradiation. Therefore, individual dosimetry is mandatory prior to treatment with radiolabeled Pentixather (Figs. 6 and 7). For a general introduction to the quantitative analysis of the biodistribution of radiopharmaceuticals, the reader is referred to the MIRD pamphlets 16 and 21 [27,28].

The purpose of dosimetry is to determine for a radiopharmaceutical the radiation absorbed doses per administered activity in the tissues of interest (Fig. 6). This is done by measuring activity time curves, i.e. the individual biokinetics of a patient, and by calculating the proportion of the administered activity that disintegrate in these tissues. As the therapeutic nuclide ^{177}Lu emits both ß$^{-}$ and γ radiation, dosimetry can be performed by scintigraphy of [^{177}Lu]Pentixather. Details on dosimetry with ^{177}Lu can be found in MIRD pamphlet 26 [29], in the following only essential points are summarized.

^{177}Lu decays with 6.65 days half-life and emits 113 and 208 keV photons suitable for scintigraphy with emission probabilities of 6.2% and 10.4% per nuclear disintegration, respectively. Often only the 208 keV photons registered in a 15%–20% energy window centered at 208 keV are used for dosimetry. The gamma camera of choice should have two camera heads equipped with medium-energy collimators and preferably thicker 5/8″ scintillation crystals instead of the standard 3/8″ crystals. Highest dosimetric accuracy can be obtained with gamma cameras capable of tomographic scintigraphy (SPECT) in combination with X-ray CT. The CT is used for morphological correlation, target volume quantification, and to correct for attenuation and scatter of the photons. SPECT images are acquired by rotating the camera heads around the patient and taking several planar images from different directions, e.g. 2×60 frames of matrix size 128×128 by rotating each camera head over in total 180° with 3° angular steps at 20–30 s acquisition time per projection. The resulting set of images is used together with the CT to calculate tomographic data which, except for a constant factor containing the measuring sensitivity of the gamma camera, reflect the most probable activity distribution in the patient's body.

Pre-therapeutic dosimetry of larger tumor lesions, kidneys, and other accumulating organs such as liver or spleen is possible with ^{177}Lu activities as low as 200 MBq. Due to inherent uncertainties, dosimetry of the red marrow remains less reliable in many patients even after the administration of much higher activities. Several measurements over 4–5 days should be performed to determine the biokinetics if [^{177}Lu]Pentixather is also used for subsequent therapy. Measurements over 3–4 days are sufficient if the patient is treated with ^{90}Y-pentixather.

^{90}Y, which has a shorter half-life of 64 h, does not emit photons which are well suited for use in dosimetry by scintigraphy,

however, the ^{90}Y kinetics can be calculated from measured ^{177}Lu data. ^{90}Y has higher ß-energy as compared to ^{177}Lu and is expected to be more nephrotoxic, but has the advantage that due to the shorter half-life, stem cells can be transplanted earlier after myeloablative treatment, thus reducing the duration of bone marrow aplasia.

The activity for treatment is determined based on the results of the pre-therapeutic dosimetry. The kidney-absorbed dose from peptide receptor radionuclide therapies should be limited to 23 Gy [30,31]. Kidney absorbed doses reported in [26] ranged from 0.5 to 3.1 Gy/GBq for [^{177}Lu]Pentixather and are expected to be about a factor of 4 higher for [^{90}Y]Pentixather. In non-myeloablative therapy, usually a dose limit of 2 Gy for the red marrow is adopted based on experience obtained in the treatment of thyroid carcinoma patients with ^{131}I [32].

2.6. CXCR4-directed radionuclide therapy

As a main achievement of the theranostic approach for individualized therapy, a peptide CXCR4 ligand which can be labelled with α- and/or β-emitters (Pentixather) has been recently developed representing a therapeutic counterpart to the diagnostic PET/SPECT agents [14,25]. Before CXCR4-directed endoradiotherapy can be considered, confirmation of sufficient target expression by means of [^{68}Ga]Pentixafor-PET/CT is mandatory. Given the high intraindividual heterogeneity of CXCR4 expression by the various myeloma lesions, a comparison to [^{18}F]FDG should be performed. Until now, endoradiotherapy (ERT) is preceded in every patient by a pre-therapeutic dosimetry study with a tracer dose of [^{177}Lu]Pentixather to exclude relevant retention in critical organs, to allow safely administrable activities and to estimate the achievable tumor doses. Assessment of estimated radiation doses to the kidneys, liver, spleen, bone marrow and – if applicable – to tumor lesions is performed by SPECT/CT and planar scintigraphy. Planar whole body scans are taken over several days and regions of interest are drawn for the organs of interest and corresponding background regions. The resulting count statistics are fitted by bi-exponential decay functions in order to approximate the activity kinetics in the organs. The fit functions are integrated and normalized to activity concentrations measured quantitatively by SPECT/CT. Based on individual dosimetry, patients are treated by intravenous injection of ^{177}Lu- or ^{90}Y-labelled Pentixather approximately 3–7 days after pre-therapeutic dosimetry. The radionuclide to be administered for ERT is chosen depending on tumor burden, biological half-life of the radiopharmaceutical and the associated time interval to stem cell transplantation (SCT).

To prevent renal toxicity, 2 L of a solution containing arginine and lysine (25 g/L each) are co-infused in analogy to the joint IAEA, EANM, and SNMMI practical guidance on peptide receptor radionuclide therapy [33]. The therapy itself is very well tolerated without any acute adverse effects. However, given the high tumor cell kill, tumor lysis syndrome has been observed in a single patient with very high tumor burden. Therefore, prophylaxis should be initiated in selected cases [34].

3. Results and discussion

3.1. CXCR4 imaging in hematologic malignancies

Feasibility of CXCR4-directed non-invasive imaging could be demonstrated for several different hematologic disorders including leukemia, lymphoma, or multiple myeloma (MM) [15,23,24,35–38]. Most experience with CXCR4-directed PET imaging has been gained in MM in which around two thirds of patients could be demonstrated to overexpress the receptor on the myeloma cell surface (Fig. 2). As for many other tumor entities, CXCR4 positivity represented a negative prognostic factor. Interestingly, patients can present with striking inter- and intra-individual receptor expression heterogeneity which has to be investigated regarding the underlying mechanisms and implication by future studies [39]. In a patient with extranodal marginal zone lymphoma of the orbital cavities displaying high CXCR4 expression, CXCR4-directed PET could also be used for response assessment which should be addressed in future studies [40]. However, receptor expression seems to be a dynamic process which can be severely influenced by preceding or concomitant chemotherapy (Fig. 7) [unpublished data]. Current investigations try to identify underlying biological implication and potential targets to exploit synergistic combinations of different treatment modalities, e.g. combinations of CXCR4 up-regulating agents prior to scheduled imaging with [^{68}Ga]Pentixafor-PET (to improve sensitivity) or chemokine-directed therapy. So far, additional [^{18}F]FDG-PET should be performed in cases with suspicion on CXCR4-negative, viable disease.

3.2. CXCR4 receptor imaging in solid cancers

Overexpression of the receptor has also been reported in various different types of solid cancers, including breast, pancreatic, ovarian and lung cancer. CXCR4 expression has been shown to correlate with negative outcome [41]. Some initial experience with non-invasive, in vivo receptor imaging using PET could be gained in some pilot studies. Vag et al. have demonstrated a rather modest receptor expression in a small hetereogenous cohort including patients with a large variety of solid cancers including pancreatic cancer, laryngeal cancer, non–small cell lung cancer, prostate cancer, melanoma, breast cancer, hepatocellular carcinoma, glioblastoma, sarcoma, or cancer of unknown primary [24]. Thus, the authors concluded that in vitro CXCR4 expression profiles of solid cancers and metastases described in the literature does not seem to sufficiently depict the in vivo distribution revealed by CXCR4-targeted PET and that the detectability of solid cancers seems to be generally lower for [^{68}Ga]Pentixafor PET than for [^{18}F]FDG PET. However, at least three solid tumor entities seem to hold potential of CXCR4-directed theranostics. In a pilot study of 10 patients with small cell lung cancer (SCLC), intense receptor expression in 8/10 subjects has been reported. CXCR4 expression of tumor lesions could be confirmed by immunohistochemistry [22]. Additionally, Bluemel at al. were able to demonstrate feasibility of [^{68}Ga]Pentixafor imaging in patients with advanced adrenocortical cancer (ACC) with 70% of patients enrolled generally qualifying for CXCR4-directed treatment [42]. Recently, Werner et al. reported on increasing receptor expression with increasing tumor grade in neuroendocrine tumors [43,44]. Thus, in the future, [^{68}Ga]Pentixafor PET/CT might serve as non-invasive read-out for evaluating the possibility of CXCR4-directed radionuclide therapies in advanced dedifferentiated SSTR-negative tumors.

3.3. CXCR4 receptor as target structure for imaging inflammation

As CXCR4 represents a relevant mediator of immune cell homing, there is a gaining interest in using CXCR4-directed probes for molecular imaging of inflammation and infection [45]. First encouraging results have been reported in models of acute myocardial infarction and ischemic stroke [23,46,47]. In the course of experimental cardiac infarction, Thackeray et al. visualized CXCR4-expressing immune cells using [^{68}Ga]Pentixafor and μPET. Regional CXCR4-upregulation in infarcted areas of the myocardium peaked after 3 days and corresponded to the presence of inflammatory cells such as macrophages and granulocytes. Of interest, co-administration of the CXCR4 antagonist Plerixafor resulted in effective blocking of tracer retention. In a preliminary patient cohort,

variable signal strength has been observed during the course of myocardial infarction and a significant correlation to respective tracer retention in the bone marrow has been shown [46]. In another preclinical study, [^{125}I]Pentixafor retention was associated to the presence of inflammatory cells in atherosclerotic plaques [48]. CXCR4-directed PET may therefore be suitable for imaging vulnerable plaques. [^{68}Ga]Pentixafor accumulation in the vessel wall of patients has also been recently shown to be associated with well-accepted risk factors of atherosclerosis [49]. Further disease models and clinical approaches of molecular imaging of inflammation in the cardiovascular system have been recently summarized [50].

3.4. CXCR4 directed therapy in hematological malignancies

First encouraging results could be obtained from small pilot studies in advanced multiple myeloma. In all patients treated so far, CXCR4-directed ERT was well-tolerated and resulted in high initial response rates [25,34]. Experience and promising data have also been gained for other hematologic malignancies beyond myeloma including relapsed or refractory acute myeloid leukemia and diffuse large B cell lymphoma on single case basis which could also be effectively targeted by radionuclide therapy. In all cases, ERT was added to standard high-dose chemotherapy as part of the conditioning regimen prior to autologous or allogeneic stem cell transplantation in order to augment tumor cell kill. In addition, stem cell rescue mediates bone marrow ablation that is also an effect of CXCR4-directed therapy due to receptor expression on tumor but also physiological bone marrow progenitor cells. In general, myeloablation can be expected at approximately 2 weeks after ERT. Therefore, ERT is especially suitable in hematologic disease in which tumor bone marrow ablation is highly desirable and stem cell rescue not a concern. Of note, use of the shorter-lived ^{90}Y has proven advantageous over ^{177}Lu due to exact interval of 14 days between ERT and SCT in comparison to the more variable outcomes of ^{177}Lu. Given the risk of infection and other complications during a prolonged phase of aplasia, most of current ERT are performed with [^{90}Y]Pentixather notwithstanding the disadvantage of insufficient post-therapeutic dosimetry due to pure β-emission.

Whereas toxicity particularly to the bone marrow have prevented the use of CXCR4-directed radionuclide therapy in solid cancers so far, this approach could be considered an option in selected malignancies including adrenocortical cancer and small cell lung cancer, given the intense receptor expression in relapsed stages. Additionally, future trials will investigate the benefit of ERT in patients with multiple myeloma or lymphoma at earlier disease stages (COLPRIT trial, Eudra-CT 2015-001817-28). Also, the use of α-particle emitters (^{225}Ac, ^{213}Bi) which have been successfully implemented in the care of patients with prostate cancer might prove beneficial in homogenously CXCR4 expressing malignancies including diffuse large B cell lymphoma or SCLC [51,52]. Future research will also focus on combinations of ERT and conventional therapies which could lead to synergistic effects. Both preclinical studies in myeloma cell lines as well as clinical observations in patients with various diseases (i.e., multiple myeloma, diffuse large B cell lymphoma, acute myeloid leukemia) have suggested the possibility to up- and/or down-regulate CXCR4 on the cell surface.

4. Conclusion

CXCR4-directed imaging and treatment using beta- or positron-emitter labeled antagonists is readily available for clinical and preclinical research. There is evidence that accumulation of [^{68}Ga]Pentixafor and similar radiopharmaceuticals closely reflect CXCR4 expression in vivo. Distinct expression patterns of CXCR4 in myeloma and other hematological neoplasms facilitate the use of [^{177}Lu]Pentixather or [^{90}Y]Pentixather for targeted radionuclide therapy. Initial results reveal an exciting therapeutic activity while exhibiting only negligible acute side effects. The CXCR4-directed theranostic approach will be assessed from 2018 in a clinical phase I-II trial (COLPRIT). Whereas most applications so far addressed oncological research, a future role of CXCR4-specific imaging is envisioned in inflammation and infection research.

Human and animal rights

All experiments and results presented in this manuscript have been carried out in accordance with the Declaration of Helsinki for experiments envolving humans. Infomred consent has been obtained from all patients undergoing imaging with [^{68}Ga]Pentixafor PET/CT. Treatment with [^{177}Lu]Pentixather or [^{90}Y]Pentixather has been offered on a compassionate use base after informed consent. Animal experiments have been carried out in accordance with the EU directive 2010/63/EU.

Acknowledgements

The authors want to thank the staff members of the "Lehrstuhl für Pharmazeutische Radiochemie", Technische Universität München, Munich, and the members of the preclinical imaging labs, Dept. of Nuclear Medicine, Technische Universität München, Munich and Dept. of Nuclear Medicine, University of Würzburg. The work was supported in part by grants from Deutsche Krebshilfe e.V. (grant 70111973), the Wilhelm Sander-Foundation and the German Research Foundation (SFB 824).

Financial support

A.K.B. and C.L. received funding from Wilhelm Sander-Foundation and Deutsche Krebshilfe e.V.; A.K.B., K.L. and H.J.W. received support from Deutsche Forschungsgemeinschaft (DFG).

Disclosures

H.J.W. is founder and shareholder of Scintomics. All other authors disclose any financial and personal relationships and declare no conflicts of interest.

References

[1] U.M. Domanska et al., A review on CXCR4/CXCL12 axis in oncology: no place to hide, Eur. J. Cancer 49 (1) (2013) 219–230.
[2] T. Nagasawa et al., Defects of B-cell lymphopoiesis and bone-marrow myelopoiesis in mice lacking the CXC chemokine PBSF/SDF-1, Nature 382 (6592) (1996) 635–638.
[3] J.A. Burger, T.J. Kipps, CXCR4: a key receptor in the crosstalk between tumor cells and their microenvironment, Blood 107 (5) (2006) 1761–1767.
[4] G.A. Donzella et al., AMD3100, a small molecule inhibitor of HIV-1 entry via the CXCR4 co-receptor, Nat. Med. 4 (1) (1998) 72–77.
[5] H.E. Broxmeyer et al., Rapid mobilization of murine and human hematopoietic stem and progenitor cells with AMD3100, a CXCR4 antagonist, J. Exp. Med. 201 (8) (2005) 1307–1318.
[6] M.R. Kuhne et al., BMS-936564/MDX-1338: a fully human anti-CXCR4 antibody induces apoptosis in vitro and shows antitumor activity in vivo in hematologic malignancies, Clin. Cancer Res. 19 (2) (2013) 357–366.
[7] A. Orimo et al., Stromal fibroblasts present in invasive human breast carcinomas promote tumor growth and angiogenesis through elevated SDF-1/CXCL12 secretion, Cell 121 (3) (2005) 335–348.
[8] A. Muller et al., Involvement of chemokine receptors in breast cancer metastasis, Nature 410 (6824) (2001) 50–56.
[9] Y. Chen et al., CXCR4 downregulation of let-7a drives chemoresistance in acute myeloid leukemia, J. Clin. Invest. 123 (6) (2013) 2395–2407.
[10] B. Nervi et al., Chemosensitization of acute myeloid leukemia (AML) following mobilization by the CXCR4 antagonist AMD3100, Blood 113 (24) (2009) 6206–6214.
[11] I.D. Weiss, O. Jacobson, Molecular imaging of chemokine receptor CXCR4, Theranostics 3 (1) (2013) 76–84.

[12] H.J. Wester et al., Disclosing the CXCR4 expression in lymphoproliferative diseases by targeted molecular imaging, Theranostics 5 (6) (2015) 618–630.
[13] E. Gourni et al., PET of CXCR4 expression by a (68)Ga-labeled highly specific targeted contrast agent, J. Nucl. Med. 52 (11) (2011) 1803–1810.
[14] M. Schottelius et al., [177Lu]pentixather: comprehensive preclinical characterization of a first CXCR4-directed endoradiotherapeutic agent, Theranostics 7 (9) (2017) 2350–2362.
[15] K. Philipp-Abbrederis et al., In vivo molecular imaging of chemokine receptor CXCR4 expression in patients with advanced multiple myeloma, EMBO Mol. Med. 7 (4) (2015) 477–487.
[16] K. Luckerath et al., Targeting paraprotein biosynthesis for non-invasive characterization of myeloma biology, PLoS One 8 (12) (2013) e84840.
[17] O. Demmer et al., Design, synthesis, and functionalization of dimeric peptides targeting chemokine receptor CXCR4, J. Med. Chem. 54 (21) (2011) 7648–7662.
[18] G.P. George et al., Preclinical evaluation of a CXCR4-specific (68)Ga-labelled TN14003 derivative for cancer PET imaging, Bioorg. Med. Chem. 22 (2) (2014) 796–803.
[19] S.V. Hartimath et al., Evaluation of N-[(11)C]methyl-AMD3465 as a PET tracer for imaging of CXCR4 receptor expression in a C6 glioma tumor model, Mol. Pharm. 11 (11) (2014) 3810–3817.
[20] G. Guan et al., CXCR4-targeted near-infrared imaging allows detection of orthotopic and metastatic human osteosarcoma in a mouse model, Sci. Rep. 5 (2015) 15244.
[21] K. Herrmann et al., Biodistribution and radiation dosimetry for the chemokine receptor CXCR4-targeting probe 68Ga-pentixafor, J. Nucl. Med. 56 (3) (2015) 410–416.
[22] C. Lapa et al., [68Ga]Pentixafor-PET/CT for imaging of chemokine receptor 4 expression in small cell lung cancer–initial experience, Oncotarget 7 (8) (2016) 9288–9295.
[23] C. Lapa et al., [(68)Ga]Pentixafor-PET/CT for imaging of chemokine receptor 4 expression after myocardial infarction, JACC Cardiovasc. Imaging 8 (12) (2015) 1466–1468.
[24] T. Vag et al., first experience with chemokine receptor CXCR4-targeted pet imaging of patients with solid cancers, J. Nucl. Med. 57 (5) (2016) 741–746.
[25] K. Herrmann et al., First-in-human experience of CXCR4-directed endoradiotherapy with 177Lu- and 90Y-labeled pentixather in advanced-stage multiple myeloma with extensive intra- and extramedullary disease, J. Nucl. Med. 57 (2) (2016) 248–251.
[26] C. Lapa et al., CXCR4-directed endoradiotherapy induces high response rates in extramedullary relapsed multiple myeloma, Theranostics 7 (6) (2017) 1589–1597.
[27] J.A. Siegel et al., MIRD pamphlet no. 16: Techniques for quantitative radiopharmaceutical biodistribution data acquisition and analysis for use in human radiation dose estimates, J. Nucl. Med. 40 (2) (1999) 37S–61S.
[28] W.E. Bolch et al., MIRD pamphlet No. 21: a generalized schema for radiopharmaceutical dosimetry – standardization of nomenclature, J. Nucl. Med. 50 (3) (2009) 477–484.
[29] M. Ljungberg et al., MIRD Pamphlet No. 26: joint EANM/MIRD guidelines for quantitative 177Lu SPECT applied for dosimetry of radiopharmaceutical therapy, J. Nucl. Med. 57 (1) (2016) 151–162.
[30] H. Bergsma et al., Subacute haematotoxicity after PRRT with (177)Lu-DOTA-octreotate: prognostic factors, incidence and course, Eur. J. Nucl. Med. Mol. Imaging 43 (3) (2016) 453–463.
[31] H. Bergsma et al., Nephrotoxicity after PRRT with (177)Lu-DOTA-octreotate, Eur. J. Nucl. Med. Mol. Imaging 43 (10) (2016) 1802–1811.
[32] M. Lassmann et al., EANM Dosimetry Committee series on standard operational procedures for pre-therapeutic dosimetry I: blood and bone marrow dosimetry in differentiated thyroid cancer therapy, Eur. J. Nucl. Med. Mol. Imaging 35 (7) (2008) 1405–1412.
[33] L. Bodei et al., The joint IAEA, EANM, and SNMMI practical guidance on peptide receptor radionuclide therapy (PRRNT) in neuroendocrine tumours, Eur. J. Nucl. Med. Mol. Imaging 40 (5) (2013) 800–816.
[34] C. Lapa, K. Herrmann, A.H. Hänscheid, K. Läckerath, M.M. SchotteliusKircher, R. A. Werner, M. Schreder, S. Samnick, S. Kropf, S. Knop, A.K. Buck, H. EInsele, H.J. Wester, K.M. Kortüm, CXCR4-directed endoradiotherapy induces high response rates in extramedullary relapsed Multiple Myeloma, Theranostics (2017).
[35] P. Herhaus et al., Targeted positron emission tomography imaging of CXCR4 expression in patients with acute myeloid leukemia, Haematologica 101 (8) (2016) 932–940.
[36] C. Bluemel et al., 68Ga-PSMA-PET/CT in patients with biochemical prostate cancer recurrence and negative 18F-choline-PET/CT, Clin. Nucl. Med. (2016).
[37] C. Lapa et al., [68Ga]Pentixafor-PET/CT for imaging of chemokine receptor 4 expression in small cell lung cancer – initial experience, Oncotarget (2016).
[38] C. Lapa et al., [68Ga]Pentixafor-PET/CT for imaging of chemokine receptor CXCR4 expression in multiple myeloma – comparison to [18F]FDG and laboratory values, Theranostics 7 (1) (2017) 205–212.
[39] C. Lapa et al., The gross picture: intraindividual tumour heterogeneity in a patient with nonsecretory multiple myeloma, Eur. J. Nucl. Med. Mol. Imaging 44 (6) (2017) 1097–1098.
[40] P. Herhaus et al., Response assessment with the CXCR4-directed positron emission tomography tracer [68Ga]Pentixafor in a patient with extranodal marginal zone lymphoma of the orbital cavities, EJNMMI Res. 7 (1) (2017) 51.
[41] D. Kaemmerer et al., Differential expression and prognostic value of the chemokine receptor CXCR4 in bronchopulmonary neuroendocrine neoplasms, Oncotarget 6 (5) (2015) 3346–3358.
[42] C. Bluemel et al., Investigating the chemokine receptor 4 as potential theranostic target in adrenocortical cancer patients, Clin. Nucl. Med. 42 (1) (2017) e29–e34.
[43] R.A. Werner et al., Imaging of chemokine receptor 4 expression in neuroendocrine tumors – a triple tracer comparative approach, Theranostics 7 (6) (2017) 1489–1498.
[44] R.A. Werner et al., Intraindividual tumor heterogeneity in NET - Further insight by C-X-C motif chemokine receptor 4-directed imaging, Eur. J. Nucl. Med. Mol. Imaging 44 (3) (2017) 553–554.
[45] T. Derlin et al., Integrating MRI and chemokine receptor CXCR4-targeted PET for detection of leukocyte infiltration in complicated urinary tract infections after kidney transplantation, J. Nucl. Med. (2017).
[46] J.T. Thackeray et al., Molecular imaging of the chemokine receptor CXCR4 after acute myocardial infarction, JACC Cardiovasc. Imaging 8 (12) (2015) 1417–1426.
[47] J.S. Schmid et al., [68Ga]pentixafor-positron emission tomography/computed tomography detects chemokine receptor CXCR4 expression after ischemic stroke, Circ. Cardiovasc. Imaging 9 (9) (2016) e005217.
[48] F. Hyafil et al., Imaging the cytokine receptor CXCR4 in atherosclerotic plaques with the radiotracer 68Ga-pentixafor for PET, J. Nucl. Med. 58 (3) (2017) 499–506.
[49] D. Weiberg et al., Clinical molecular imaging of chemokine receptor CXCR4 expression in atherosclerotic plaque using 68ga-pentixafor PET: correlation with cardiovascular risk factors and calcified plaque burden, J. Nucl. Med. (2017).
[50] M. Kircher, C. Lapa, Novel noninvasive nuclear medicine imaging techniques for cardiac inflammation, Curr. Cardiovasc. Imaging Rep. 10 (2) (2017) 6.
[51] C. Kratochwil et al., 225Ac-PSMA-617 for PSMA-targeted alpha-radiation therapy of metastatic castration-resistant prostate cancer, J. Nucl. Med. 57 (12) (2016) 1941–1944.
[52] M. Sathekge et al., 213Bi-PSMA-617 targeted alpha-radionuclide therapy in metastatic castration-resistant prostate cancer, Eur. J. Nucl. Med. Mol. Imaging 44 (6) (2017) 1099–1100.